Research article

Enhancing terminal erythroid differentiation in human embryonic stem cells through TRIB3 overexpression

Xiaoling Wang [1], Tiantian Cui [1], Hao Yan, Lingping Zhao, Ruge Zang, Hongyu Li, Haiyang Wang, Biao Zhang, Junnian Zhou, Yiming Liu, Wen Yue, Jiafei Xi [*], Xuetao Pei [**]

Beijing Institute of Radiation Medicine, Beijing, 100850, PR China

A R T I C L E   I N F O

A B S T R A C T

Tribbles pseudokinase 3 (TRIB3) expression significantly increases during terminal erythropoiesis in vivo. However, we found that TRIB3 expression remained relatively low during human embryonic stem cell (hESC) erythropoiesis, particularly in the late stage, where it is typically active. TRIB3 was expressed in megakaryocyte-erythrocyte progenitor cells and its low expression was necessary for megakaryocyte differentiation. Thus, we proposed that the high expression during late stage of erythropoiesis could be the clue for promotion of maturation of hESC-derived erythroid cells. To our knowledge, the role of TRIB3 in the late stage of erythropoiesis remains ambiguous. To address this, we generated inducible TRIB3 overexpression hESCs, named TRIB3$^{\text{tet-on OE}}$ H9, based on a Tet-On system. Then, we analyzed hemoglobin expression, condensed chromosomes, organelle clearance, and enucleation with or without doxycycline treatment. TRIB3$^{\text{tet-on OE}}$ H9 cells generated erythrocytes with a high proportion of orthochromatic erythroblast in flow cytometry, enhanced hemoglobin and related protein expression in Western blot, decreased nuclear area size, promoted enucleation rate, decreased lysosome and mitochondria number, more colocalization of LC3 with LAMP1 (lysosome marker) and TOM20 (mitochondria marker) and up-regulated mitophagy-related protein expression after treatment with 2 μg/mL doxycycline. Our results showed that TRIB3 overexpression during terminal erythropoiesis may promote the maturation of erythroid cells. Therefore, our study delineates the role of TRIB3 in terminal erythropoiesis, and reveals TRIB3 as a key regulator of UPS and downstream mitophagy by ensuring appropriate mitochondrial clearance during the compaction of chromatin.

1. Introduction

Tribbles pseudokinase 3 (TRIB3) is a pseudokinase, which has a kinase domain that lacks enzyme activity, that binds to a variety of proteins in eukaryotic cells, and mediates the development of diabetes and various cancers [1–8]. Additionally, TRIB3 acts as a stress protein; its expression is up-regulated in response to multiple stressors, and it directly interacts with the cargo receptor P62, thereby

---

interfering with its binding to LC3 and ubiquitinated substrate proteins, which suppresses autophagic flux and protects several tumor-promoting factors from autophagic degradation in cancer cells [9,10]. TRIB3 was reported to interact with E3 ubiquitin ligases, such as SMURF1 and COP1, thereby targeting proteins for degradation and acting as a negative modulator of megakaryocytopoiesis in megakaryocyte-erythrocyte progenitor (MEP) cells via the ERK pathway [11–13]. Our previous work give us a strong hint that TRIB3 took part in the maturation of erythroid cells [14]. However, the role of TRIB3 in terminal erythropoiesis and the underlying molecular mechanisms have not yet been elucidated.

Pluripotent stem cells (PSCs) are one of the most promising cell source to generate red blood cells (RBCs) for transfusion due to their theoretically unlimited capable of self-renewal. Many groups have attempted to obtain hPSC-derived RBCs that can be utilized to lessen the dependence on blood donations. They generated hESC-derived RBCs that highly expressed embryonic globin chains, with a <20 % enucleation rate [15–20]. However, further optimization is necessary for the production of more mature RBCs that are suitable for human RBC transfusion. Erythroblast development involves pro-erythroblasts (Pro-E), basophilic erythroblasts (Baso-E), poly-chromatic erythroblasts (Poly-E), and orthochromatic erythroblasts (Ortho-E), which then generate mature RBCs. These four populations have distinct morphologies and gene markers that enable their isolation and identification [21,22]. Maturation of erythroid
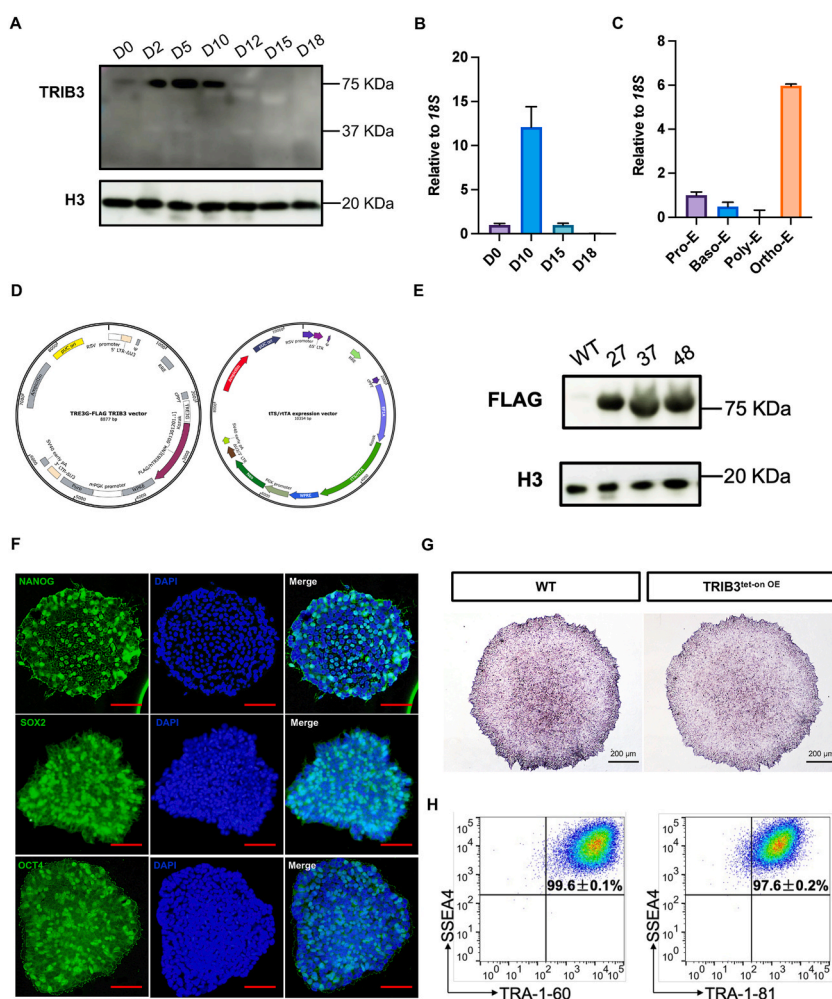
Fig. 1. Establishment of inducible TRIB3-overexpressing H9 cell line

(A) Western blot showing TRIB3 expression during H9 erythropoiesis on D0, D2, D5, D10, D12, D15, and D18, with Histone3 (H3) serving as a reference. (B) RT-qPCR showing TRIB3 expression in erythroblasts during H9 erythropoiesis on D0, D10, D15, and D18, with *18S* serving as a reference. (C) RT-qPCR showing TRIB3 expression in umbilical cord blood-CD34 cell-derived erythroblasts, with *18S* as a reference. Pro-E: pro-erythroblasts; Baso-E: basophilic erythroblasts; Poly-E: polychromatic erythroblasts; Ortho-E: orthochromatic erythroblasts. (D) Dual vector system used to establish the inducible overexpression embryonic stem cell line. (E) Western blot showing TRIB3 expression in TRIB3[tet-on OE] H9 after treatment with 2 μg/mL doxycycline, with H3 as a reference. (F) Immunofluorescent assay of NANOG, SOX2, and OCT4 expression in TRIB3[tet-on OE] H9 cells. Each line on the DAPI (blue), NANOG/OCT4/SOX2 (green), and merge shows cells with pluripotent stem marker expression. Bar = 100 μm. (G) Alkaline phosphatase live staining of TRIB3[tet-on OE] H9 and WT H9 cells. Bar = 200 μm. (H) Flow cytometry showing SSEA4/TRA-1-60 and SSEA4/TRA-1-81 expression in TRIB3[tet-on OE] H9 cells. (For interpretation of the references to colour in this figure legend, the reader is referred to the Web version of this article.)

cells entails a series of well-coordinated events, e.g., hemoglobin accumulation and switching, chromosome condensing, organelle clearance, membrane remodeling, and enucleation. During differentiation, several proteins exhibited regularity expression, including transferrin receptor (TFRC; CD71), glycophorin A (GYPA; CD235a), α4-intergrin, and solute carrier family 4 member 1 (SLC4A1; BAND3) [21]. Meanwhile, the morphology of erythroblasts undergoes sequential changes, observed using cytospin stanning and transmission electron microscopy (TEM); for instance, mitochondria are progressively cleared with a significant difference in numbers between Poly-E (13.3 $\pm$ 0.6 mitochondrial sections per cell) and Ortho-E (4.28 $\pm$ 0.43 mitochondrial sections per cell) cells in umbilical cord blood (UCB) CD34$^+$cell derived erythroblasts, and the nucleus area decreased from 78 $\pm$ 9 % in Poly-E cells, to 42 $\pm$ 3 % in Ortho-E cells compared to that in Pro-E cells [22]. Hemoglobin switching is driven by BCL11A, ZBTB7A, LIN28B, and SOX6, which silence gamma-globin genes and promote beta-globin gene expression during the maturation of erythroid cells [23–26]. The absence of beta-globin in PSC-derived erythroid cells were basically due to their primitive erythropoiesis development mode, i.e., absent of primitive isotype of master regulator BCL11A [14,27,28]. And impaired pyrenocyte extrude could be due to their short of master regulator UBE2O which driven chromosome condensation, enucleation and large scale degradation of the cell contents by ubiquitination [14,29–32]. This suggests that targeting pivotal regulators of hemoglobin switching, cell content degradation, e.g., organelle and nuclear clearance, may be a promising strategy for improving the efficacy of RBC production in vitro.

The clearance of mitochondria by mitophagy is the most studied model of organelle clearance in terminal erythropoiesis. Mitophagy primarily acts as a mitochondrial quality control mechanism required for the removal of damaged and dysfunctional mitochondria [33], or for mitochondria that are completely functional but not necessary for particular cell types, such as erythrocytes. Reticulocytes undergo intense intracellular remodeling to form mature erythrocytes, predominantly through UBE2O, PINK1 and PARK2 etc. regulators mediated Ubiquitin-Proteasome System (UPS) and downstream mitophagy [31,34–37]. Notably, the molecular mechanism of programmed mitophagy activation during cell development and differentiation differs from that of quality control mitophagy and depends on selective autophagy receptors. BCL2/adenovirus E1B 19-kDa-interacting protein 3-like (BNIP3L/NIX) is a selective receptor that plays a central role in mammalian terminal erythropoiesis [38,39]. Nix (−/−) mice develop anemia with a reduced number of mature erythrocytes and compensatory increase in erythroid precursors for defective entry of mitochondria into autophagosomes for clearance [40]. The sphingosine-1-phosphate pathway, outer mitochondrial membrane protein translocator protein, voltage dependent anion channels, and the core autophagy gene ATG4A were reported to promote terminal erythropoiesis via mitophagy [37,41–43]. TRIB3 interacts with the autophagy protein P62, which had been reported to mediate the ubiquitination in parkin (PINK1 and PARK2 etc.)-independent mitophagy [44,45]. Therefore we hypothesized that TRIB3 is involved in terminal erythropoiesis induced by UPS and downstream mitophagy.

Here, we established an embryonic stem cell line with inducible overexpression of TRIB3, TRIB3$^{tet-on\ OE}$ H9, to explore the role of TRIB3 in terminal erythropoiesis. We observed that the TRIB3$^{tet-on\ OE}$ H9-derived erythroid cells treated with doxycycline (DOX+) exhibited enhanced terminal differentiation, hemoglobin expression, chromosome condensation, and mitochondrial clearance compared with those in the DOX-group (without DOX). Functional studies confirmed maturation stage-specific regulation of mitophagy during erythroid maturation and demonstrated a critical role for TRIB3 in the regulation of terminal differentiation and UPS-mitophagy regulated organelle clearance in maturing erythroblasts. Taken together, our findings reveal important insights into the mechanisms that regulate terminal erythroid maturation and provide a novel paradigm for understanding normal and perturbed erythropoiesis.

2. Results

2.1. TRIB3$^{tet-on\ OE}$ H9 cells overexpressed TRIB3 after DOX treatment

TRIB3 expression is significantly up-regulated in the late stage of erythropoiesis, especially in Poly-E and Ortho-E. Our data showed that TRIB3 expression was relatively low during the maturation of H9-derived erythroid cells (Fig. 1A–B). While the expression of TRIB3 heightened in umbilical cord blood (UCB)-CD34 cell derived erythroblast cells (Fig. 1C). To explore the role of TRIB3 in terminal erythropoiesis, we constructed a dual vector to induce TRIB3 overexpression based on a tet-on system (Fig. 1D, Fig. S1A). The selected clones treated with 2 μg/mL DOX showed various degrees of up-regulated TRIB3 expression, determined by western blotting; therefore, 2 μg/mL DOX was chosen for further experiments (Fig. 1E). Positive clones presented a conical, round embryonic stem cell morphology; and expressed the pluripotent markers NANOG, SOX2, and OCT4, determined by immunofluorescence assay (Figure S1B; Fig. 1F). Live staining showed that cell clones expressed the characteristic stem cell marker alkaline phosphatase (Fig. 1G). Furthermore, flow cytometry demonstrated that most of the selected clones were double positive for SSEA4 & TRA1-60 and SSEA4 & TRA1-81 (Fig. 1H). Overall, we established and validated an embryonic stem cell line with inducible TRIB3 overexpression using H9 based on a Tet-on system.

2.2. Terminal erythropoiesis and hemoglobin expression in human erythroid cells were promoted by TRIB3 overexpression

To study erythroid differentiation of TRIB3$^{tet-on\ OE}$ H9 cells with and without DOX, we analyzed the proportions of Pro-E, Baso-E, Poly-E and Ortho-E cells during erythropoiesis as described previously [21]. To integrate the low expression of TRIB3 during terminal erythropoiesis (Fig. 1B) and our erythropoiesis progression model, we treated H9-derived erythroid cells with 2 μg/mL DOX (DOX+) from day (D) 6 to D18. Our erythroid development model ran for 18 days, and Pro-E and Baso-E were the dominant cell types on D12, while Poly-E and Ortho-E were predominant on D15 and D18, respectively (Fig. 2A). The data showed different percentage distributions between TRIB3$^{tet-on\ OE}$ H9-derived erythroid cells with DOX (DOX+) and without DOX (DOX-). Erythroblasts derived from

DOX + cells were more highly distributed in the more mature populations, Poly-E and Ortho-E, than those from the DOX-group (Fig. 2B). Moreover, the DOX + group had a higher mean fluorescence intensity (MFI) for the erythroid-specific protein GPA and a higher percentage of the mature erythroblast population CD71⁻ GPA⁺ (Fig. 2C–D). These data suggest that TRIB3 overexpression promotes the maturation of H9-derived erythroid cells; therefore, we compared the expression of the functional protein hemoglobin between DOX- and DOX + on D10, D12, D15, and D18. Western blot showed that H9-derived erythroid cells treated with DOX exhibited significantly upregulated HBA, HBB, and HBG expression, and increased expression of transcription factors (TFs) involved in hemoglobin switching, such as ZBTB7A, BCL11A, and SOX6, but deceased expression of the suppressor of hemoglobin switching, LIN28B (Fig. 2E). We also observed that the expression of TFs related to the maturation of erythroid cells, including TAL1, MXI1,
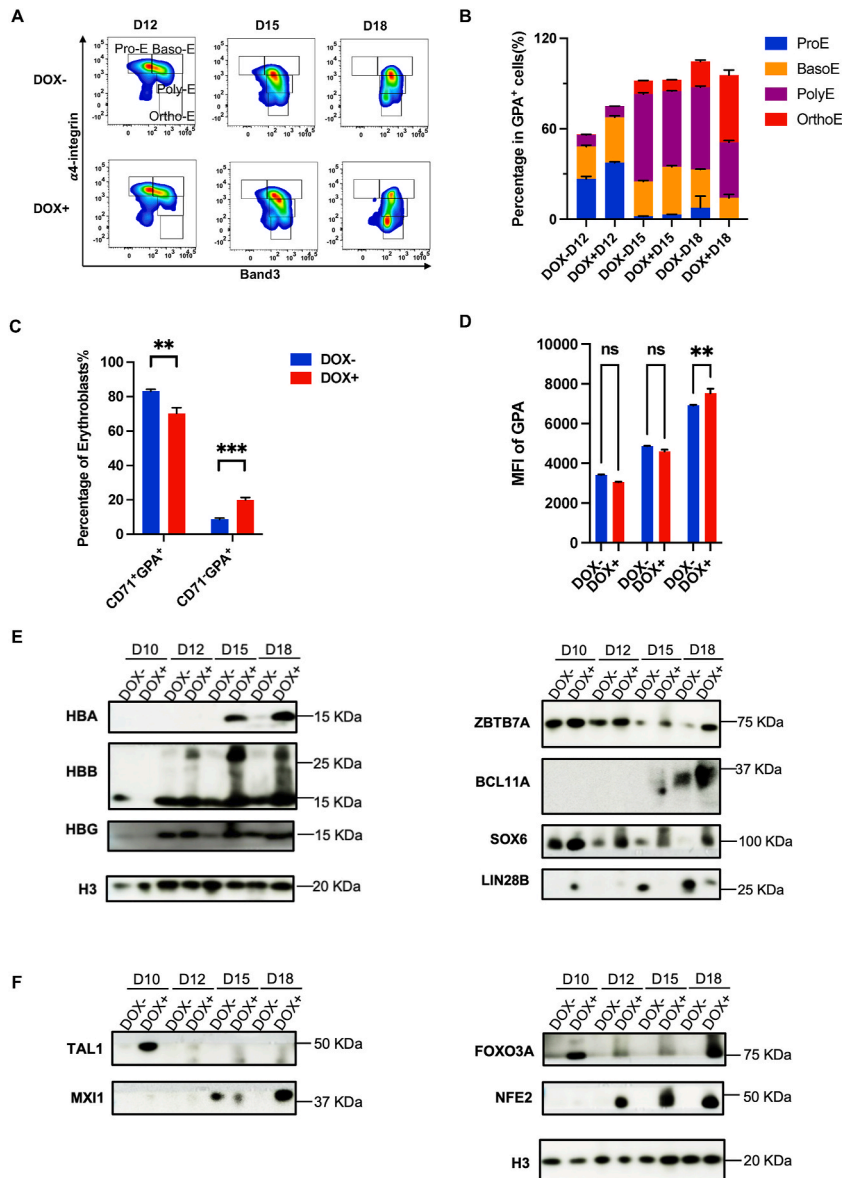
Fig. 2. TRIB3 overexpression is beneficial for differentiation and hemoglobin expression of human erythroid cells
(A) Representative flow cytometry analysis of band3 and α4-integrin expression on TRIB3^tet-on OE H9 cells treated with 2 μg/mL doxycycline since D6 (DOX+) and without doxycycline (DOX-) cell-derived GPA⁺ erythroblasts. (B) Quantitative analyses of erythroblasts at distinct developmental stages based on the expression of band3 and α4-integrin in Fig. 2A. Data are from 3 experimental replicates and values are mean ± SEM. (C) Representative flow cytometry analysis of CD71 and GPA expression on hESC-derived erythroid cells in the DOX+ and DOX-groups. (D) Quantitative analysis of mean fluorescent intensity (MFI) of GPA on TRIB3^tet-on OE H9 cells treated with or without 2 μg/mL DOX in D12, D15, D18. (E–F) Western blot of ES-derived erythroid cells treated from D6 with the indicated DOX doses and those from the DOX-group. Protein levels of HBA, HBB, HBG, ZBTB7A, BCL11A, SOX6, and LIN28B are shown in E, and those of TAL1, MXI1, FOXO3A, and NFE2 are shown in F; H3 was used as a loading control.

FOXO3A, and NFE2, was dramatically increased in the DOX + group (Fig. 2F). While there was no significant difference between terminal erythropoiesis related protein in DOX treat group of wild type (WT) H9 cells and WT (Fig. S2C). Hence, there was no WT with DOX group included in this work hereafter. Collectively, these findings suggest that TRIB3 overexpression not only enhances hemoglobin expression but also may promote enucleation of H9-derived erythroid cells.

2.3. Enhanced chromatin condensation in TRIB3-overexpressing polychromatic and orthochromatic erythroblasts

During terminal erythropoiesis in Pro-E, Baso-E, Poly-E and Ortho-E, cells undergo gradual nuclear condensation that is associated with decreased cell size. Then, extrusion of the pyknotic nucleus occurs in the final stage of erythropoiesis, which involves highly regulated asymmetric cell division [46]. To compare the differentiation process between two groups, we sorted erythroblasts into four groups, and observed four morphologically distinct populations (Fig. 3B, Fig. S2A). Based on this strategy, we compared the nuclear areas of Poly-E and Ortho-E between the DOX- and DOX + groups using a cytospin and image flow cytometry test (Fig. 3A–C). The nuclear areas of Poly-E and Ortho-E in the DOX + group were significantly decreased compared to those in the DOX-group (Fig. 3D), the data of nuclear area comparison between two group by immunofluorescent test was consistent with image flow cytometry data (Fig. 3E, F, I). Which suggests that TRIB3 overexpression promoted nuclear condensation of embryonic stem cell (ES)-derived erythroid cells. Therefore, we compared the enucleation rates between two groups; ES-derived erythroid cells generated few mature RBCs (Fig. S2B), while the DOX + group generated a significantly higher number of enucleated erythroblasts (Fig. 3G–H). In summary, comparison of the nuclear area and enucleation rate between DOX- and DOX+, based on erythroblast analysis and DRAQ5 staining, indicated that TRIB3 overexpression not only promotes nuclear condensation and enucleation in H9-derived erythroid cells, but also increases other cell contents and activity, such as mitochondrial degradation.

2.4. TRIB3 overexpression improves the mitochondrial clearance of human erythroid cells

Given the significant role of TRIB3 in the condensation of chromatin, we next investigated whether it is also involved in organelle clearance during reticulocyte maturation. First, we sorted the present cell populations by distinct morphology characteristics, determined by TEM images (Fig. 4A–B, Fig. S3A). As described previously, mitochondria were significantly cleared from the Poly-E to Ortho-E stages in UCB-CD34$^+$ derived erythroblasts [22]. In our data, yellow line-marked mitochondrial sections in Poly-E and Ortho-E of the DOX + group decreased compared to those in the DOX-group (Fig. 4A, B and E). Then, we stained lysosomes and mitochondria in cultured Poly-E (left panel) and Ortho-E (right panel) and observed a decrease in mitochondria with overexpression of TRIB3 (Fig. 4C, F). Consistent with the TEM images and immunofluorescence assays, flow cytometry results revealed a significant increase in the number of mitochondria in TRIB3-expressing Poly-E, which underwent mitophagy, then the number of mitochondria was significantly decreased in Ortho-E (Fig. 4D, E, G and H). Together, these results imply that TRIB3 expression leads to enhanced mitochondrial clearance in late-stage erythroblasts. Mitochondria are involved in metabolism and energy consumption, and erythropoiesis is highly associated with the reprogramming of glucose metabolism and energy consumption [47]. Furthermore, we also observed that mitochondria from Baso-E to Ortho-E acquired a round shape (Fig. S3B), which suggests that there were changes in the metabolic state and large-scale degradation of mitochondria during terminal erythropoiesis. To investigate this, we examined whether TRIB3 overexpression influenced energy metabolism in H9-derived erythroid cells. ES-derived erythroid cells were treated with 2 μg/mL DOX from D6, and then collected on D18 for oxygen consumption rate (OCR) assays. OCR levels indicated the occurrence of mitochondrial respiration. DOX-induced TRIB3 overexpression influenced mitochondrial respiration parameters in ES-derived erythroid cells (Fig. 4I). Compared to that in control cells, TRIB3 overexpression-induced erythroid differentiation not only decreased basal and maximal mitochondrial respiration rates, but also reduced ATP production, proton leaks and non-mitochondrial oxygen consumption (Fig. 4J–K, Figs. S4A–D). To further confirm the effect of TRIB3 on terminal erythropoiesis, we treated cells with DOX on D10, D15 and D6, then performed an OCR assay on D18 (Fig. S4E). Basal and maximal mitochondrial respiration and ATP production on D10 and D15 were reduced compared to those on D6 after treatment, while proton leak and spare respiration showed no significant difference (Figs. S4F–H). Which supports that D6 was the optimal time for DOX treatment. These results indicated that TRIB3 promotes mitochondrial clearance and, subsequently, the modulation of cellular bioenergetics during erythroid differentiation.

2.5. TRIB3 overexpression promotes mitophagy in human erythroid cells

TRIB3 interacts with the well-known autophagy protein P62 to mediate downstream autophagy signaling in liver fibrosis [10], and mitophagy (a type of autophagy) is prevalent in terminal erythropoiesis by intercellular mitochondrial transfer [48,49]. Given the significance of TRIB3 in the terminal differentiation and chromosome condensation of erythroid cells, we next investigated whether its role in organelle clearance is dependent on mitophagy during reticulocyte maturation. To further determine whether overexpression of TRIB3 affects organelle clearance through mitophagy, we first determined the number of lysosome contain mitochondria using TEM. As shown in Fig. 5A–B, mitochondria with distinct cristae architecture were surrounded by lysosomes in the DOX + group, while blank lysosomes were predominant in the DOX-group. The number of lysosomes with mitochondria inside in the DOX + group was significantly higher than that in the DOX-group (Fig. 5F). Next, we compared the expression of the autophagy marker LC3 with that of the mitochondrial marker TOM20 and lysosome marker LAMP1 between DOX- and DOX + on D15, when Baso-E and Poly-E were predominant in the cultured erythroblasts. As Fig. 5C and D shows, we observed that LC3 and LAMP1 and LC3 and TOM20 were colocalized in the DOX+ and DOX-groups, respectively. Moreover, the co-localization of LC3 and LAMP1 and LC3 and TOM20 was significantly higher in the DOX + group than that in the DOX-group (Fig. 5G–H). UBE2O is involved in the enucleation of erythroid

cells and serves as master regulator of enucleation by ubiquitin and downstream mitophagy-mediated degradation [31]. Western blot showed that the ubiquitin-related UBE2O, autophagy-related ATG5, ATG7, P62, and LC3B, the mitophagy-related PINK1 and PARK2 were significantly up-regulated in DOX + group than that in the DOX-group (Fig. 5E). Consistent with Fig. S2C, there was no significant
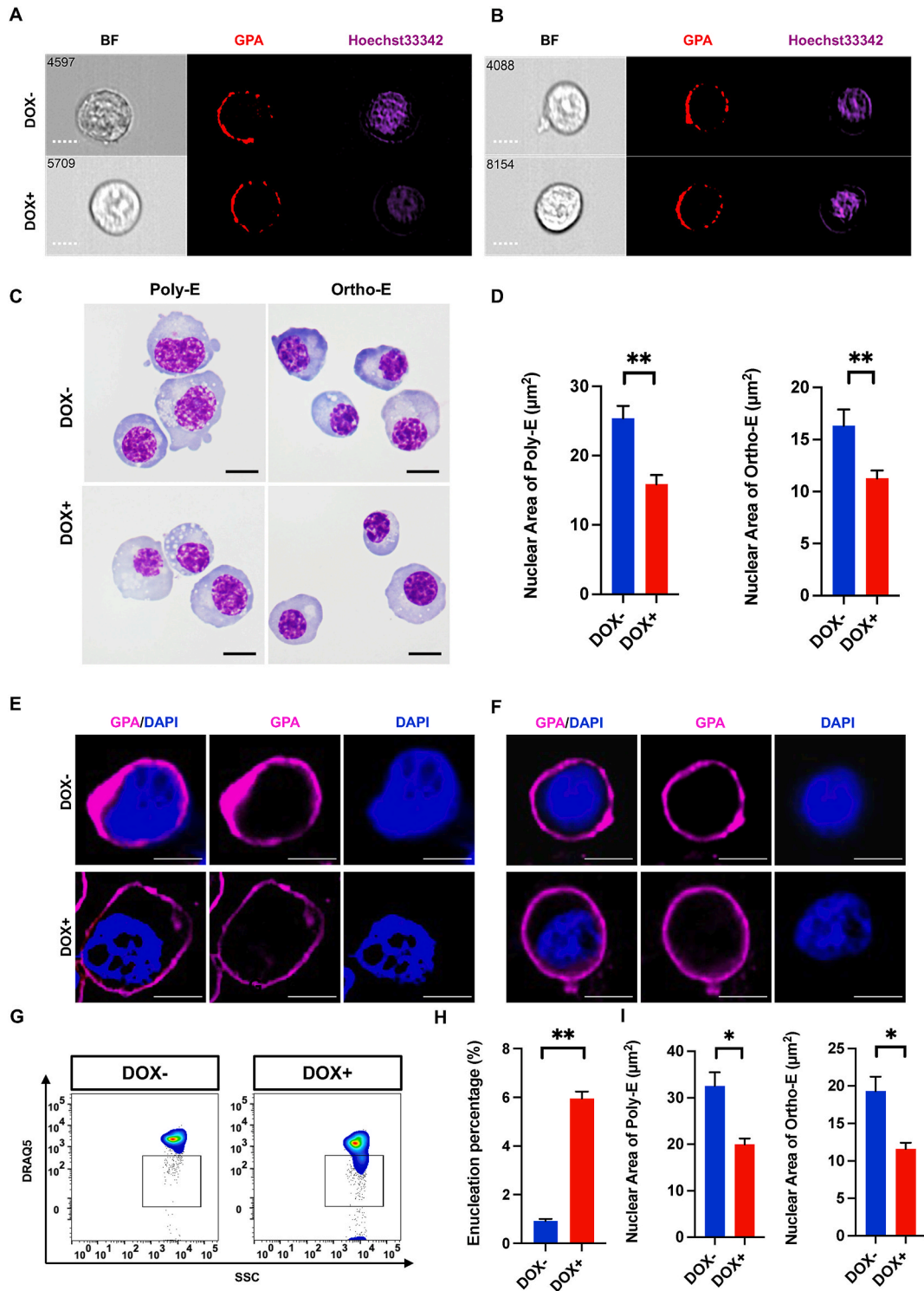
(caption on next page)

Fig. 3. TRIB3 overexpression is beneficial for nuclear condensation and hemoglobin expression of human erythroid cells
(A-B) Representative ImageStream images of polychromatic erythroblasts (Poly-E) and orthochromatic erythroblasts (Ortho-E). GPA-labeled Poly-E (A) and Ortho-E (B) showing different nuclear area sizes in the DOX+ (lower line) and DOX- (upper line) groups, Bar = 7 μm. (C) Composite representative cytospin images of FAC-sorted TRIB3$^{tet-on\ OE}$ H9 cells generating Poly and Ortho erythroblasts in the DOX+ (lower line) and DOX-(upper line) groups. (D) Quantitative analyses of nuclear area (μm^2) of Poly and Ortho erythroblasts by ImageStream in Fig. 3A, n = 3. **p < 0.01. (E–F) Representative immunofluorescence images of Poly-E (E) and Ortho-E (F) in the DOX+ (lower line) and DOX- (upper line) groups. GPA (magenta)-labeled Poly-E and Ortho-E showing different nuclear area (marked with DAPI as blue) sizes in the DOX+ (lower line) and DOX- (upper line) groups. (G) Representative flow cytometry analyses of enucleation as assessed by DRAQ5 staining in D18. (H) Quantitative analyses of enucleation in Fig. 3G, n = 3. **p < 0.01. (I) Quantitative analyses of nuclear area (μm^2) of Poly and Ortho erythroblasts by immunofluorescent in Fig. 3E–F n = 3. *p < 0.05. (For interpretation of the references to colour in this figure legend, the reader is referred to the Web version of this article.)

difference between autophagy related protein expression in DOX treat group of wild type (WT) H9 cells and WT (Fig. S4I). This data all suggests that TRIB3 promotes mitochondrial clearance could through UPS and downstream mitophagy.

3. Discussion

Considering the dramatic increase of IRIB3 in the late stage of erythroblast in UCB cells, while barely expression during H9 derived terminal erythropoiesis of cells. To explore the role of TRIB3 in terminal erythropoiesis, here we established an embryonic stem cell line with inducible overexpression of TRIB3, TRIB3$^{tet-on\ OE}$. We compared terminal differentiation, hemoglobin expression, nuclear condensation, enucleation, and mitochondrial clearance between TRIB3$^{tet-on\ OE}$-derived erythroid cells with and without DOX treatment. TRIB3 overexpression enhances terminal erythropoiesis through previously mentioned mechanisms by promoting the expression of master TFs and mitophagy. To our knowledge, this is the first report of the role of TRIB3 in terminal erythropoiesis in vitro.

During erythropoiesis, autophagy results in the loss of erythroid organelles. Yang et al., 2022 reported that mitochondrial transfer occurred from early stage erythroblasts to murine erythroblastic island macrophages. Hence they proposed that canonical autophagy predominantly mediates mitochondrial clearance during the early stages of terminal differentiation, whereas non-canonical mitophagy pathways dominate the late stages of erythroid maturation [49]. While approximately 2 % of wild-type mice have some erythrocytes bearing mitochondria, in conditionally Atg7-deleted mice, this increases to 40 % of erythrocytes [35]. Mutation of the mitochondrial DNA polymerase Polg disrupts the link between iron uptake and mitochondrial clearance, leading to the circulation of erythrocytes with mitochondria and subsequent significant hematological problems [50]. Here, we also observed sequential changes in transcription activity of several macroautophagy-related genes and non-canonical mitophagy genes, then gradual reduction in the expression of lysosome-related genes from the early to late stages of erythroblasts (Fig. S5). The outer mitochondrial membrane protein voltage-dependent anion channel-1 is involved in human erythroblast terminal differentiation by regulating mitochondrial clearance during in vivo terminal erythropoiesis [51]. mDia2 and Yippee-like 4 were reported to promote mouse RBC membrane integrity [29, 30]. This supports our observation of enlarged RBCs in the DOX-group (Fig. S3C); therefore, we propose that TRIB3 overexpression also promotes membrane integrity during terminal erythropoiesis.

TRIB3-mediated cell proliferation has been well documented in different kinds of cancers [10,52,53], which makes targeting TRIB3 or its interaction with P62 a promising clinical treatment strategy. TRIB3 interacts with several TFs, such as FOXO1, SOX2, or ATF4, in breast cancer and regulates the stress response [54,55]. Intriguingly, here, we found that various master TFs were activated after the induction of TRIB3 overexpression, which suggests that TRIB3 may be involved in the upstream regulation of terminal erythropoiesis. Li et al. reported that the enrichment of long-range interactions between heterochromatin and the erythroid master regulators GATA1 and KLF1 is pivotal during terminal erythropoiesis [40]. Besides direct interaction with P62, TRIB3 may recruit various master TFs through long-range interactions with heterochromatin in terminal erythropoiesis. In the present work, we found that overexpression of TRIB3 enhanced the protein expression levels of TAL1, MXI1, FOXO3A, UBE2O, and NFE2. TAL1 is essential for the complete progression of the erythroid lineage and is required from the progenitor stage to the final stages of differentiation. Later in hemopoietic differentiation, continued TAL1 expression is critical for erythroid maturation, as a lack of TAL1 leads to inhibition of erythropoiesis [56,57]. In contrast, FOXO3A, UBE2O, MXI1 and NFE2 are involved in the late stages, primarily affecting early matured erythrocytes [58–61]. NFE2 directly interacts with the autophagy genes NIX and ULK1 to participate in terminal erythropoiesis [62]. UBE2O is involved in proteome remodeling through the programmed elimination of most generic constituents of the cell during reticulocyte maturation, even non-erythroid cells, e.g., 293 cells [31]. Thus, while these results clearly support the conclusion that TRIB3 enhances terminal erythropoiesis, they do not highlight which regulators or pathways of the process are promoted. In this context, the findings of a recent study indicated that TRIB3 recruits the tripartite motif, containing eight bases, to form an E3 ligase complex that mediates ER stress-induced HNF4α degradation in liver disease [63]. TRIB3, TRIB2, and TRIB1 can all bind to the ubiquitin ligase COP1 [64]. TRIB3 attenuates adipocyte differentiation by promoting COP1-mediated ubiquitination and degradation of acetyl-coenzyme A carboxylase-1 [13]. Thus, whether TRIB3 might additionally act as an important E3 ubiquitin ligase adaptor within erythroblasts during terminal erythropoiesis is requires further investigation, as this may contribute to the effects of TRIB3 on erythrocyte maturation.

The proportion of arrested erythroid cells at the G1 stage of the cell cycle is increased in NFE2-deficient mice, and TAL1 is also involved in cell cycle exit [57,62]. Given that the degradation of the cell contents during the maturation of erythroid cells is primarily mediated by ubiquitin and large scale degradation of nuclei and organelles, our results are also compatible with the possibility that TRIB3 may be involved in terminal erythropoiesis via the ubiquitin system. Therefore, analysis of whether TRIB3 expression affects cell
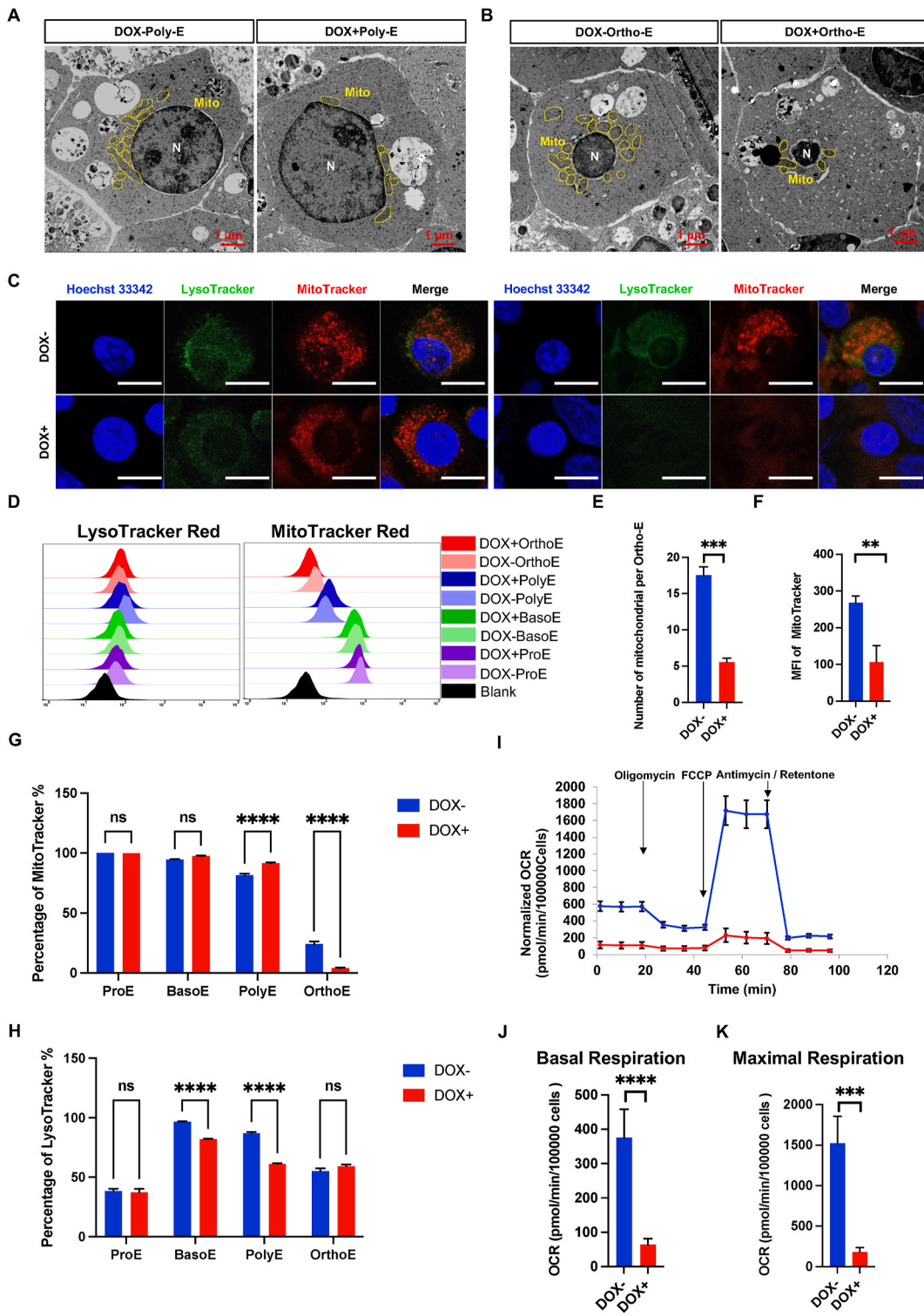
(caption on next page)

Fig. 4. Mitochondria mass is altered upon TRIB3 upregulation

(A-B) Increased mitochondrial clearance in ES-derived erythroblasts was determined by transmission electron microscopy (TEM). Analysis of mitochondria in erythroid cells generated from the DOX- and DOX + groups was undertaken using a TEM. Number of mitochondria was determined by morphology characteristics. (C) TRIB3 overexpression promotes mitophagy clearance in TRIB3[tet-on OE] H9-derived erythroblasts. After treatment with doxycycline (2 μg/mL) for the indicated times, ES-derived erythroblasts were stained with LysoTracker green (100 nM), MitoTracker red (200 nM), and Hoechst 33342 (2 μg/mL); the mitochondrial morphology was observed using a fluorescence microscope. Magnification: × 630; Bar = 10 μm. (D) TRIB3 overexpression promotes lysosome and mitochondria clearance in TRIB3[tet-on OE] H9-derived erythroblasts. Lysosome mass and mitochondria mass were tested by LysoTracker red and MitoTracker red in GPA; band3 and α4-integrin define Pro-E, Baso-E, Poly-E, and Ortho-E cells, respectively. (E) Quantitative analyses of number of mitochondria in Ortho erythroblasts of DOX- and DOX + by TEM in Fig. 4A–B. Data are presented as mean ± SEM. n = 3. ***p < 0.001. (F) Quantitative analysis of MFI of MitoTracker on TRIB3[tet-on OE] H9 cell-derived Ortho-E with or without 2 μg/mL DOX. Data are presented as mean ± SEM. n = 3. **p < 0.01. (G–H) Percentage of MitoTracker (G) and LysoTracker (H) in Fig. 4D. Data are presented as mean ± SEM. n = 3. ns: non-significant, p > 0.05; ****p < 0.0001. (I) OCR profile of TRIB3[tet-on OE] H9-derived D18 cells treated with 2 μg/mL DOX from D6 (red line, n = 5) and no DOX (blue line, n = 4). Quantified data are presented as means ± SEM. Cells were sequentially treated with 0.5 μm oligomycin, 1 μm FCCP, and 2 μm rotenone/antimycin A at the indicted time points. (J–K) Basal respiration (J) and maximal respiration (K) were determined by calculating average values for each phase of erythroid cells in Fig. 4I. Data are presented as mean ± SEM. ***p < 0.001; ****p < 0.0001. (For interpretation of the references to colour in this figure legend, the reader is referred to the Web version of this article.)

content clearance by ubiquitination under the conditions of experimentally-induced stress erythropoiesis could be beneficial. Given that differentiation and proliferation of erythroid cells are interlinked, sharing common energy origins and overlapping signal transduction pathways, our results are also compatible with the possibility that TRIB3 may be involved in the regulation of cell fate decisions at the erythroblast stage for maturation and proliferation. Mechanistic studies further illustrated that TRIB3 controls cell-fate decisions of mesenchymal stem cells via cooperative activation of BMP/Smad and Wnt/beta-catenin signaling, two major signals that govern skeletal development and bone formation [65]. TRIB3 is also involved in cell proliferation in various diseases [66–69], but there are few reports on its role in cell differentiation. Our data identified TRIB3 as a pivotal regulator in the maturation of erythroid cells. Therefore, it would also be interesting to analyze the pathways or regulators that interact with TRIB3 to alter the balance between terminal erythropoiesis and cell proliferation.

In this study, we observed a positive regulatory role for TRIB3 in the late stage of erythroid differentiation during hESC-derived cell erythropoiesis without the wild type (WT) H9 treat with DOX group. Our data also indicated that the observed organelle clearance was due to mitophagy and upstream UPS, and the upregulated hemoglobin expression was related to the higher TF expression. However, the overall enucleation rate was far away to close to the in vivo level, and more solid evidence is required to confirm the mechanism by which TRIB3 enhances the maturation of erythroid cells. In this context, an in vivo model with inducible TRIB3 overexpression could provide more details. Indeed, it was previously published that DOX is able to induce a shift metabolism toward a more glycolytic phenotype in various human cancer cell line [70] and induce mitophagy in porcine enterocytes [71]. Whilst, the treatment of 2 μg/mL DOX in human induced pluripotent stem cell showing no effect on Cas9 protein expression [72], DOX has been used extensively in inducible overexpression system to establish pluripotent stem cell lines and in gene function studies [73–75]. Together with our check about the effect of DOX on the maturation of PSC derived erythroid cells before our study and there were no significant differences between WT and WT with DOX, we decided not to include WT with DOX group in this work. While the further detection of the precise DOX effect on human stem cells could provide details about more robust inducible overexpression system in regenerative medicine research.

In conclusion, here, we show that TRIB3 overexpression is involved in the late stage of erythroid differentiation. We also report a higher distribution of Ortho-E, higher expression of hemoglobin and related proteins, and decreased lysosome and mitochondria after TRIB3 overexpression during terminal erythropoiesis. Further, mitophagy-related lysosome with mitochondria inside and colocalization of LC3, an organelle marker, with the well-known mitophagy proteins PINK1 and PARK2 were upregulated. These findings could aid the development of a new strategy for RBC production from ES using engineered cell lines without risks, and provide new insights into the role of mitophagy in terminal erythropoiesis.

4. Methods

4.1. Samples

Human umbilical cord blood (UCB) was acquired from the Umbilical Cord Blood Bank, Beijing, China. All procedures involving human subjects in this study were approved by Ethics Committee of the AMMS (Approval No.: AF/SC-08/02.160).

4.2. Generation of erythrocyte from UCB-CD34+ cells

Human UCB-CD34+ cells were isolated and purified by CD34 MicroBead Kit (Mitenyi Biotech, Bergisch Gladbach, DE) as the manufacturer's instructions. Erythroid production from UCB-CD34+ cells were based on previously reported [21].
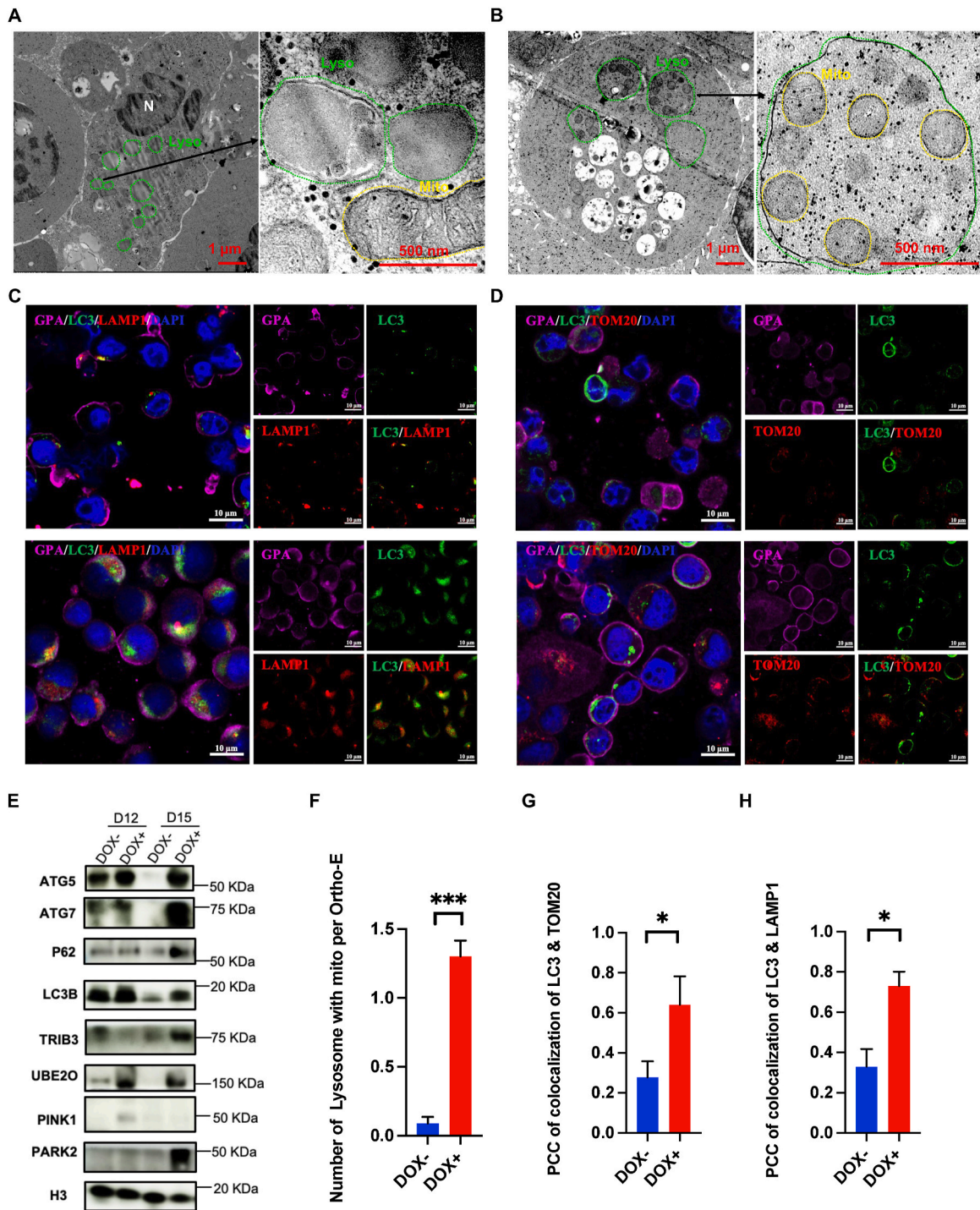
Fig. 5. Mitophagy is enhanced in TRIB3-overexpressing erythroid cells

(A-B) Increased lysosome fusion with mitochondria in DOX-induced TRIB3-overexpressing Ortho-E. Ultrastructural analysis of erythroid cells derived from ES (DOX+, B) and wild type group (DOX-, A) was performed for lysosomes (marked with green line) with mitochondria (marked with yellow line) in erythroid subpopulations using transmission electron microscopy. High magnification of electron micrographs for Ortho-E in the DOX+ and DOX-groups is shown in the right column. The illustration was captured and analyzed for the number of individual lysosomes with mitochondria and total Ortho-E cell number using ZEISS ZEN software. N, nucleus; Mito, mitochondria; Lyso, lysosome. (C–D) Colocalization of LC3 with lysosomes and mitochondria in Poly-E (C) Ortho-E (D) as determined using an immunofluorescent microscope. Erythroid cells (marked with GPA as magenta) from ES were stained with LC3 using an immunofluorescence assay to determine LC3 (green) colocalization with mitochondria (marked with TOM20 as red) and lysosomes (marked with LAMP1 as red) in the DOX+ (upper row) and DOX- (lower row)groups. (E) Western blot

of ES-derived erythroid cells from the DOX+ and DOX-groups on D12 and D15. Protein levels of ATG5, ATG7, P62, LC3B, TRIB3, PINK1, PARK2, and UBE2O were determined, and H3 was used as a loading control. (F) Quantitative analysis of lysosome fusion with mitochondria per total cell ratio in Fig. 5A–B is presented as mean ± SEM. n=3. ***p < 0.001. (G–H) Quantitative analysis of colocalization of LC3B with LAMP1 and LC3B with TOM20 in Ortho-E of DOX+ and DOX- by confocal microscopy in Fig. 5C-D n = 3. *p < 0.05. (For interpretation of the references to colour in this figure legend, the reader is referred to the Web version of this article.)

4.3. Establishment of inducible TRIB3-overexpressing H9 cells

H9 cells were cultured in Matrigel® (Corning, Corning, NY, USA) coated plates and supplied with mTeSR™ Plus medium (STEMCELL Technologies, Vancouver, CA, USA), and the medium was replaced every two days. H9 cells were transfected with lentivirus (MOI = 5, VectorBuilder, Chicago, IL, US), as per the manufacturer's guidelines. Clones positive for the lentivirus were selected using 1 μg/mL puromycin and then confirmed by overexpression test. Then, TRIB3 overexpression was induced by 2 μg/mL DOX treatment.

4.4. Erythrocyte production from H9 cells

H9 cells were passaged after being dissolved in ReLeSR™ (STEMCELL Technologies) when they reached 80 % confluence. Then, 2–3 days before erythroid induction, H9 cells were passaged to reach 90 % confluence. The day before erythroid induction, H9 cells were dissolved in ACCUTASE™ (STEMCELL Technologies) to produce a single cell suspension, then cultured in sequential culture medium, as previously described, to generate erythroid cells [76].

4.5. Antibody staining, FACS, and flow cytometry

A total of 1×10^6 cells were prepared for flow cytometry analysis. GPA-BV421, α4-intergrin-APC (BD), BAND3-FITC (ARP, Dietzenbach, DE), GPA-BV421, CD71-FITC (BD), and DRAQ5-APC (CST, Charlotte, NC, USA) were incubated with the cells at 4 °C for 30 min after blocking with 4 % AB serum, and then the protein expression was analyzed after washing once with phosphate-buffered saline (PBS). Relative cell populations were stained by GPA-BV421, α4-intergrin-APC (BD), and BAND3-FITC (ARP) as described before and then sorted by FACS Aria II (BD, Franklin Lakes, NJ, USA) as previously reported [21]. Data were analyzed using Flowjo (BD).

4.6. Real-time PCR

Cells were rinsed in Trizol reagent (Invitrogen, Carlsbad, CA, USA) to extract total RNA, which was reverse-transcribed to cDNA using qPCR Master Mix (Toyobo, Osaka, Osaka, JP), as per the manufacturer's instructions. To determine gene expression levels during erythropoiesis, real-time PCR was applied based on the primers listed in Table S1. Data were analyzed using Prism (GraphPad, Boston, MA, USA).

4.7. Western blot

First, ACCUTASE™-dissolved cells or cells removed from medium were washed in cooled PBS, and then lysed in radio-immunoprecipitation assay buffer (Thermo Fisher, Waltham, MA, USA) with proteinase inhibitors (Thermo Fisher) on ice for 30 min. Total protein was obtained by centrifugation of the cell suspension at 12000 g for 30 min. The sample input was quantified using a bicinchoninic acid (BCA) kit (Thermo Fisher). Equal amounts of protein were boiled with 100 μM DTT (Thermo Fisher) and loading buffer (Bio-Rad, Hercules, CA, USA) at 95 °C for 10 min, then loaded onto an SDS-PAGE gel (Tsingke, Beijing, Beijing, China), and a standard marker (Bio-Rad) was loaded as the running marker. SDS-PAGE was performed in MOPS running buffer (Tsingke, Beijing, Beijing, China) at 150 V for 70–90 min to separate proteins, which were transferred from the gel to polyvinylidene difluoride membranes in transfer buffer (Bio-Rad). After blocking with skim milk and incubation with antibodies, H3, TRIB3, FLAG, HBA, HBB, HBG, GPA, PINK1, PARK2, (abcam, Branford, CT, USA), ZBTB7A, BCL11A, SOX6, LIN28B, TAL1, MXI1, FOXO3A, UBE2O, NFE2, P62, ATG5, ATG7 (abclone, Wuhan, Hubei, China), and LC3B (Thermo Fisher) signals were measured after adding Pierce™ ECL Western Blotting Substrate (Thermo Fisher).

4.8. Cytospin preparation

First, $0.5–1 \times 10^5$ cells in 100 μL cooled PBS were used to prepare cytospin preparations on coated slides, using the CYTOPRO® cytocentrifuge at 300 g for 3 min (ELITechGroup, Puteaux, FR). The slides were fixed and cooled, then stained with May-Grunwald (BASO, Zhuhai, Guangdong, China) solution A for 1 min, rinsed in water for 90 s, and subsequently stained with Giemsa solution B (BASO) for 10 min, then washed with water. Image of the stained cells were captured using the Leica DM2000 inverted microscope.

4.9. Image flow cytometry

Cells were washed twice with cooled PBS and 0.1 % bovine serum albumin (BSA), then $0.5–1 \times 10^7$ cells were stained with a 1:500 dilution antibody solution for Band3-FITC (ARP, Waltham, MA, USA), CD49d-APC, CD235a-PerCP (BD, Franklin Lakes, NJ, USA), and 2 µg/mL Hoechst 33342 (Thermo Fisher). Cells were imaged using the ImageStreamX Amnis (Merck Millipore, Burlington, MA, USA) and analyzed with IDEAS (Merck Millipore).

4.10. Immunofluorescence staining

Cultured cells were fixed with 4 % paraformaldehyde for 15 min, washed with cooled PBS and 0.1 % BSA, permeabilized with 0.1 % Triton-100, blocked with 10 % donkey serum, then stained with a 1:200 dilution of primary antibodies for LC3B (abcam, Branford, CT, USA) and LAMP1 (abcam), as well as TOM20 (abcam), and related secondary antibodies. Samples were covered with mounting medium after being stained with 10 µM DAPI (Invitrogen, Carlsbad, CA, USA). Live cells were directly stained with 200 nM Mito-Tracker Red (beyotime, Shanghai, Shanghai, China), 100 nM LysoTracker Green (beyotime) and 2 µg/mL Hoechst 33342 (Thermo Fisher) right before observation.

4.11. Transmission electron microscopy

Approximately 6–7 million sorted erythroblast cells were immediately fixed and mounted on copper grids for testing, and then stained with lead citrate and uranyl acetate. Images of the sections were captured with a 110 kV transmission electron microscope (HT7800, Hitachi, Tokyo, JP). At least 12 images per replicates were obtained and analyzed using FIJI software. The morphological characteristics of mitochondria were analyzed, and the nuclear area of cells was calculated by FIJI software.

4.12. Statistical tests

Erythroid differentiation experiments were performed in triplicate to achieve a satisfactory correlation with the results of individual experiments. Statistical analyses were performed using Prism 8 (GraphPad, Boston, MA, US). Data were evaluated using Mann–Whitney or Kruskal–Wallis tests, and a p-value <0.05 was considered statistically significant.

Ethics statement

All procedures involving human subjects in this study were approved by Ethics Committee of the AMMS (Approval No.: AF/SC-08/02.160).

Data availability statement

The data that support the findings of this study are available from the corresponding author upon reasonable request

CRediT authorship contribution statement

Xiaoling Wang: Writing – review & editing, Writing – original draft, Visualization, Data curation, Conceptualization. **Tiantian Cui:** Data curation, Conceptualization. **Hao Yan:** Methodology. **Lingping Zhao:** Supervision, Project administration, Funding acquisition. **Ruge Zang:** Funding acquisition. **Hongyu Li:** Visualization, Methodology. **Haiyang Wang:** Investigation. **Biao Zhang:** Resources. **Junnian Zhou:** Validation. **Yiming Liu:** Resources, Formal analysis. **Wen Yue:** Project administration. **Jiafei Xi:** Writing – review & editing, Project administration. **Xuetao Pei:** Validation, Project administration, Conceptualization.

Declaration of competing interest

The authors declare that they have no known competing financial interests or personal relationships that could have appeared to influence the work reported in this paper.

Acknowledgements

Appendix A. Supplementary data

Supplementary data to this article can be found online at https://doi.org/10.1016/j.heliyon.2024.e37463.

References

[1] M. Wu, L.-G. Xu, Z. Zhai, H.-B. Shu, SINK is a p65-interacting negative regulator of NF-kappaB-dependent transcription, J. Biol. Chem. 278 (2003) 27072–27079.

[2] K. Du, S. Herzig, R.N. Kulkarni, M. Montminy, TRB3: a tribbles homolog that inhibits Akt/PKB activation by insulin in liver, Science (New York, NY) 300 (2003) 1574–1577.

[3] H.-J. Koh, D.E. Arnolds, N. Fujii, T.T. Tran, M.J. Rogers, N. Jessen, Y. Li, C.W. Liew, R.C. Ho, M.F. Hirshman, R.N. Kulkarni, C.R. Kahn, L.J. Goodyear, Skeletal muscle-selective knockout of LKB1 increases insulin sensitivity, improves glucose homeostasis, and decreases TRB3, Mol. Cell Biol. 26 (2006) 8217–8227.

[4] O. Bezy, C. Vernochet, S. Gesta, S.R. Farmer, C.R. Kahn, TRB3 blocks adipocyte differentiation through the inhibition of C/EBPbeta transcriptional activity, Mol. Cell Biol. 27 (2007) 6818–6831.

[5] N. Ohoka, S. Yoshii, T. Hattori, K. Onozaki, H. Hayashi, TRB3, a novel ER stress-inducible gene, is induced via ATF4-CHOP pathway and is involved in cell death, EMBO J. 24 (2005) 1243–1255.

[6] F. Hua, R. Mu, J. Liu, J. Xue, Z. Wang, H. Lin, H. Yang, X. Chen, Z. Hu, TRB3 interacts with SMAD3 promoting tumor cell migration and invasion, J. Cell Sci. 124 (2011) 3235–3246.

[7] M. Tomcik, K. Palumbo-Zerr, P. Zerr, B. Sumova, J. Avouac, C. Dees, A. Distler, R. Becvar, O. Distler, G. Schett, L. Senolt, J.H.W. Distler, Tribbles homologue 3 stimulates canonical TGF-β signalling to regulate fibroblast activation and tissue fibrosis, Ann. Rheum. Dis. 75 (2016) 609–616.

[8] J. Izrailit, H.K. Berman, A. Datti, J.L. Wrana, M. Reedijk, High throughput kinase inhibitor screens reveal TRB3 and MAPK-ERK/TGFβ pathways as fundamental Notch regulators in breast cancer, Proc. Natl. Acad. Sci. U. S. A 110 (2013) 1714–1719.

[9] F. Hua, K. Li, J.-J. Yu, X.-X. Lv, J. Yan, X.-W. Zhang, W. Sun, H. Lin, S. Shang, F. Wang, B. Cui, R. Mu, B. Huang, J.-D. Jiang, Z.-W. Hu, TRB3 links insulin/IGF to tumour promotion by interacting with p62 and impeding autophagic/proteasomal degradations, Nat. Commun. 6 (2015) 7951.

[10] X.-W. Zhang, J.-C. Zhou, D. Peng, F. Hua, K. Li, J.-J. Yu, X.-X. Lv, B. Cui, S.-S. Liu, J.-M. Yu, F. Wang, C.-C. Jin, Z.-N. Yang, C.-X. Zhao, X.-Y. Hou, B. Huang, Z.-W. Hu, Disrupting the TRIB3-SQSTM1 interaction reduces liver fibrosis by restoring autophagy and suppressing exosome-mediated HSC activation, Autophagy 16 (2020) 782–796.

[11] L. Butcher, M. Ahluwalia, T. Örd, J. Johnston, R.H. Morris, E. Kiss-Toth, T. Örd, J.D. Erusalimsky, Evidence for a role of TRIB3 in the regulation of megakaryocytopoiesis, Sci. Rep. 7 (2017) 6684.

[12] M.C. Chan, P.H. Nguyen, B.N. Davis, N. Ohoka, H. Hayashi, K. Du, G. Lagna, A. Hata, A novel regulatory mechanism of the bone morphogenetic protein (BMP) signaling pathway involving the carboxyl-terminal tail domain of BMP type II receptor, Mol. Cell Biol. 27 (2007) 5776–5789.

[13] L. Qi, J.E. Heredia, J.Y. Altarejos, R. Screaton, N. Goebel, S. Niessen, I.X. Macleod, C.W. Liew, R.N. Kulkarni, J. Bain, C. Newgard, M. Nelson, R.M. Evans, J. Yates, M. Montminy, TRB3 links the E3 ubiquitin ligase COP1 to lipid metabolism, Science (New York, NY) 312 (2006) 1763–1766.

[14] X. Wang, W. Zhang, S. Zhao, H. Yan, Z. Xin, T. Cui, R. Zang, L. Zhao, H. Wang, J. Zhou, X. Li, W. Yue, J. Xi, Z. Zhang, X. Fang, X. Pei, Decoding human in vitro terminal erythropoiesis originating from umbilical cord blood mononuclear cells and pluripotent stem cells, Cell Prolif. (2024) e13614.

[15] E.N. Olivier, C. Qiu, M. Velho, R.E. Hirsch, E.E. Bouhassira, Large-scale production of embryonic red blood cells from human embryonic stem cells, Exp. Hematol. 34 (2006) 1635–1642.

[16] J.J. Haro-Mora, N. Uchida, S. Demirci, Q. Wang, J. Zou, J.F. Tisdale, Biallelic correction of sickle cell disease-derived induced pluripotent stem cells (iPSCs) confirmed at the protein level through serum-free iPS-sac/erythroid differentiation, Stem Cells Translational Medicine 9 (2020) 590–602.

[17] N. Uchida, J.J. Haro-Mora, A. Fujita, D.-Y. Lee, T. Winkler, M.M. Hsieh, J.F. Tisdale, Efficient generation of β-globin-expressing erythroid cells using stromal cell-derived induced pluripotent stem cells from patients with sickle cell disease, Stem Cells (Dayton, Ohio) 35 (2017) 586–596.

[18] I. Dorn, K. Klich, M.J. Arauzo-Bravo, M. Radstaak, S. Santourlidis, F. Ghanjati, T.F. Radke, O.E. Psathaki, G. Hargus, J. Kramer, M. Einhaus, J.B. Kim, G. Kögler, P. Wernet, H.R. Schöler, P. Schlenke, H. Zaehres, Erythroid differentiation of human induced pluripotent stem cells is independent of donor cell type of origin, Haematologica 100 (2015) 32–41.

[19] J. Roh, S. Kim, J.-W. Cheong, S.-H. Jeon, H.-K. Kim, M.J. Kim, H.O. Kim, Erythroid differentiation of induced pluripotent stem cells Co-cultured with OP9 cells for diagnostic purposes, Annals of Laboratory Medicine 42 (2022) 457–466.

[20] E.N. Olivier, S. Zhang, Z. Yan, S. Suzuka, K. Roberts, K. Wang, E.E. Bouhassira, PSC-RED and MNC-RED: albumin-free and low-transferrin robust erythroid differentiation protocols to produce human enucleated red blood cells, Exp. Hematol. 75 (2019).

[21] J. Hu, J. Liu, F. Xue, G. Halverson, M. Reid, A. Guo, L. Chen, A. Raza, N. Galili, J. Jaffray, J. Lane, J.A. Chasis, N. Taylor, N. Mohandas, X. An, Isolation and functional characterization of human erythroblasts at distinct stages: implications for understanding of normal and disordered erythropoiesis in vivo, Blood 121 (2013) 3246–3253.

[22] A. Dussouchaud, J. Jacob, C. Secq, J.-M. Verbavatz, M. Moras, J. Larghero, C.M. Fader, M.A. Ostuni, S.D. Lefevre, Transmission electron microscopy to follow ultrastructural modifications of erythroblasts upon ex vivo human erythropoiesis, Front. Physiol. 12 (2021) 791691.

[23] N. Liu, S. Xu, Q. Yao, Q. Zhu, Y. Kai, J.Y. Hsu, P. Sakon, L. Pinello, G.-C. Yuan, D.E. Bauer, S.H. Orkin, Transcription factor competition at the γ-globin promoters controls hemoglobin switching, Nat. Genet. 53 (2021) 511–520.

[24] Y. Shen, J.M. Verboon, Y. Zhang, N. Liu, Y.J. Kim, S. Marglous, S.K. Nandakumar, R.A. Voit, C. Fiorini, A. Ejaz, A. Basak, S.H. Orkin, J. Xu, V.G. Sankaran, A unified model of human hemoglobin switching through single-cell genome editing, Nat. Commun. 12 (2021) 4991.

[25] A. Basak, M. Munschauer, C.A. Lareau, K.E. Montbleau, J.C. Ulirsch, C.R. Hartigan, M. Schenone, J. Lian, Y. Wang, Y. Huang, X. Wu, L. Gehrke, C.M. Rice, X. An, H.A. Christou, N. Mohandas, S.A. Carr, J.-J. Chen, S.H. Orkin, E.S. Lander, V.G. Sankaran, Control of human hemoglobin switching by LIN28B-mediated regulation of BCL11A translation, Nat. Genet. 52 (2020) 138–145.

[26] O. Sripichai, C.M. Kiefer, N.V. Bhanu, T. Tanno, S.-J. Noh, S.-H. Goh, J.E. Russell, C.L. Rognerud, C.-N. Ou, P.A. Oneal, E.R. Meier, N.M. Gantt, C. Byrnes, Y. T. Lee, A. Dean, J.L. Miller, Cytokine-mediated increases in fetal hemoglobin are associated with globin gene histone modification and transcription factor reprogramming, Blood 114 (2009) 2299–2306.

[27] K.-H. Chang, A.M. Nelson, H. Cao, L. Wang, B. Nakamoto, C.B. Ware, T. Papayannopoulou, Definitive-like erythroid cells derived from human embryonic stem cells coexpress high levels of embryonic and fetal globins with little or no adult globin, Blood 108 (2006) 1515–1523.

[28] C. Qiu, E.N. Olivier, M. Velho, E.E. Bouhassira, Globin switches in yolk sac-like primitive and fetal-like definitive red blood cells produced from human embryonic stem cells, Blood 111 (2008) 2400–2408.

[29] Y. Liu, Y. Mei, X. Han, F.V. Korobova, M.A. Prado, J. Yang, Z. Peng, J.A. Paulo, S.P. Gygi, D. Finley, P. Ji, Membrane skeleton modulates erythroid proteome remodeling and organelle clearance, Blood 137 (2021) 398–409.

[30] A. Mattebo, T. Sen, M. Jassinskaja, I. Prieto González-Albo, A.G. Alattar, R. Ramakrishnan, S. Lang, M. Järås, J. Hansson, S. Soneji, S. Singbrant, E. van den Akker, J. Flygare, Yippee like 4 (Ypel4) is essential for normal mouse red blood cell membrane integrity, Sci. Rep. 11 (2021) 15898.

[31] A.T. Nguyen, M.A. Prado, P.J. Schmidt, A.K. Sendamarai, J.T. Wilson-Grady, M. Min, D.R. Campagna, G. Tian, Y. Shi, V. Dederer, M. Kawan, N. Kuehnle, J. A. Paulo, Y. Yao, M.J. Weiss, M.J. Justice, S.P. Gygi, M.D. Fleming, D. Finley, UBE2O remodels the proteome during terminal erythroid differentiation, Science (New York, NY) (2017) 357.

[32] J. Wu, K. Moriwaki, T. Asuka, R. Nakai, S. Kanda, M. Taniguchi, T. Sugiyama, S.-I. Yoshimura, T. Kunii, T. Nagasawa, N. Hosen, A. Miyoshi, A. Harada, EHBP1L1, an apicobasal polarity regulator, is critical for nuclear polarization during enucleation of erythroblasts, Blood Advances 7 (2023) 3382–3394.

[33] K. Palikaras, E. Lionaki, N. Tavernarakis, Mechanisms of mitophagy in cellular homeostasis, physiology and pathology, Nat. Cell Biol. 20 (2018) 1013–1022.

[34] M.J. Koury, S.T. Koury, P. Kopsombut, M.C. Bondurant, In vitro maturation of nascent reticulocytes to erythrocytes, Blood 105 (2005) 2168–2174.

[35] M. Mortensen, D.J.P. Ferguson, M. Edelmann, B. Kessler, K.J. Morten, M. Komatsu, A.K. Simon, Loss of autophagy in erythroid cells leads to defective removal of mitochondria and severe anemia in vivo, Proc. Natl. Acad. Sci. U. S. A 107 (2010) 832–837.

[36] E. Ovchynnikova, F. Aglialoro, M. von Lindern, E. van den Akker, The shape shifting story of reticulocyte maturation, Front. Physiol. 9 (2018) 829.

[37] M. Moras, C. Hattab, P. Gonzalez-Menendez, S. Martino, J. Larghero, C. Le Van Kim, S. Kinet, N. Taylor, S.D. Lefevre, M.A. Ostuni, Downregulation of mitochondrial TSPO inhibits mitophagy and reduces enucleation during human terminal erythropoiesis, Int. J. Mol. Sci. 21 (2020).

[38] R.L. Schweers, J. Zhang, M.S. Randall, M.R. Loyd, W. Li, F.C. Dorsey, M. Kundu, J.T. Opferman, J.L. Cleveland, J.L. Miller, P.A. Ney, NIX is required for programmed mitochondrial clearance during reticulocyte maturation, Proc. Natl. Acad. Sci. U. S. A 104 (2007) 19500–19505.

[39] H. Sandoval, P. Thiagarajan, S.K. Dasgupta, A. Schumacher, J.T. Prchal, M. Chen, J. Wang, Essential role for Nix in autophagic maturation of erythroid cells, Nature 454 (2008) 232–235.

[40] D. Li, F. Wu, S. Zhou, X.-J. Huang, H.-Y. Lee, Heterochromatin rewiring and domain disruption-mediated chromatin compaction during erythropoiesis, Nat. Struct. Mol. Biol. 30 (2023) 463–474.

[41] C. Yang, M. Hashimoto, Q.X.X. Lin, D.Q. Tan, T. Suda, Sphingosine-1-phosphate signaling modulates terminal erythroid differentiation through the regulation of mitophagy, Exp. Hematol. 72 (2019).

[42] M.C. Stolla, A. Reilly, R. Bergantinos, S. Stewart, N. Thom, C.A. Clough, R.C. Wellington, R. Stolitenko, J.L. Abkowitz, S. Doulatov, ATG4A regulates human erythroid maturation and mitochondrial clearance, Blood Advances 6 (2022) 3579–3589.

[43] V.M.S. Betin, B.K. Singleton, S.F. Parsons, D.J. Anstee, J.D. Lane, Autophagy facilitates organelle clearance during differentiation of human erythroblasts: evidence for a role for ATG4 paralogs during autophagosome maturation, Autophagy 9 (2013) 881–893.

[44] T. Yamada, D. Murata, Y. Adachi, K. Itoh, S. Kameoka, A. Igarashi, T. Kato, Y. Araki, R.L. Huganir, T.M. Dawson, T. Yanagawa, K. Okamoto, M. Iijima, H. Sesaki, Mitochondrial stasis reveals p62-mediated ubiquitination in parkin-independent mitophagy and mitigates nonalcoholic fatty liver disease, Cell Metabol. 28 (2018).

[45] S. Geisler, K.M. Holmström, D. Skujat, F.C. Fiesel, O.C. Rothfuss, P.J. Kahle, W. Springer, PINK1/Parkin-mediated mitophagy is dependent on VDAC1 and p62/SQSTM1, Nat. Cell Biol. 12 (2010) 119–131.

[46] P. Ji, S.R. Jayapal, H.F. Lodish, Enucleation of cultured mouse fetal erythroblasts requires Rac GTPases and mDia2, Nat. Cell Biol. 10 (2008) 314–321.

[47] A. Richard, E. Vallin, C. Romestaing, D. Roussel, O. Gandrillon, S. Gonin-Giraud, Erythroid differentiation displays a peak of energy consumption concomitant with glycolytic metabolism rearrangements, PLoS One 14 (2019) e0221472.

[48] C. Yang, R. Yokomori, L.H. Chua, S.H. Tan, D.Q. Tan, K. Miharada, T. Sanda, T. Suda, Mitochondria transfer mediates stress erythropoiesis by altering the bioenergetic profiles of early erythroblasts through CD47, J. Exp. Med. 219 (2022).

[49] C. Yang, M. Endoh, D.Q. Tan, A. Nakamura-Ishizu, Y. Takihara, T. Matsumura, T. Suda, Mitochondria transfer from early stages of erythroblasts to their macrophage niche via tunnelling nanotubes, Br. J. Haematol. 193 (2021) 1260–1274.

[50] K.J. Ahlqvist, S. Leoncini, A. Pecorelli, S.B. Wortmann, S. Ahola, S. Forsström, R. Guerranti, C. De Felice, J. Smeitink, L. Ciccoli, R.H. Hämäläinen, A. Suomalainen, MtDNA mutagenesis impairs elimination of mitochondria during erythroid maturation leading to enhanced erythrocyte destruction, Nat. Commun. 6 (2015) 6494.

[51] M. Moras, C. Hattab, P. Gonzalez-Menendez, C.M. Fader, M. Dussiot, J. Larghero, C. Le Van Kim, S. Kinet, N. Taylor, S.D. Lefevre, M.A. Ostuni, Human erythroid differentiation requires VDAC1-mediated mitochondrial clearance, Haematologica 107 (2022) 167–177.

[52] P. Shen, T.-Y. Zhang, S.-Y. Wang, TRIB3 promotes oral squamous cell carcinoma cell proliferation by activating the AKT signaling pathway, Exp. Ther. Med. 21 (2021) 313.

[53] B. Hong, J. Zhou, K. Ma, J. Zhang, H. Xie, K. Zhang, L. Li, L. Cai, N. Zhang, Z. Zhang, K. Gong, TRIB3 promotes the proliferation and invasion of renal cell carcinoma cells via activating MAPK signaling pathway, Int. J. Biol. Sci. 15 (2019) 587–597.

[54] C. Jousse, C. Deval, A.-C. Maurin, L. Parry, Y. Chérasse, C. Chaveroux, R. Lefloch, P. Lenormand, A. Bruhat, P. Fafournoux, TRB3 inhibits the transcriptional activation of stress-regulated genes by a negative feedback on the ATF4 pathway, J. Biol. Chem. 282 (2007) 15851–15861.

[55] J.-M. Yu, W. Sun, Z.-H. Wang, X. Liang, F. Hua, K. Li, X.-X. Lv, X.-W. Zhang, Y.-Y. Liu, J.-J. Yu, S.-S. Liu, S. Shang, F. Wang, Z.-N. Yang, C.-X. Zhao, X.-Y. Hou, P.-P. Li, B. Huang, B. Cui, Z.-W. Hu, TRIB3 supports breast cancer stemness by suppressing FOXO1 degradation and enhancing SOX2 transcription, Nat. Commun. 10 (2019) 5720.

[56] M.P. McCormack, M.A. Hall, S.M. Schoenwaelder, Q. Zhao, S. Ellis, J.A. Prentice, A.J. Clarke, N.J. Slater, J.M. Salmon, S.P. Jackson, S.M. Jane, D.J. Curtis, A critical role for the transcription factor Scl in platelet production during stress thrombopoiesis, Blood 108 (2006) 2248–2256.

[57] Y.N. Serina Secanechia, I. Bergiers, M. Rogon, C. Arnold, N. Descostes, S. Le, N. López-Anguita, K. Ganter, C. Kapsali, L. Bouilleau, A. Gut, A. Uzuotaite, A. Aliyeva, J.B. Zaugg, C. Lancrin, Identifying a novel role for the master regulator Tal1 in the endothelial to hematopoietic transition, Sci. Rep. 12 (2022) 16974.

[58] R. Liang, G. Campreciós, Y. Kou, K. McGrath, R. Nowak, S. Catherman, C.L. Bigarella, P. Rimmelé, X. Zhang, M.N. Gnanapragasam, J.J. Bieker, D. Papatsenko, A. Ma`ayan, E. Bresnick, V. Fowler, J. Palis, S. Ghaffari, A systems approach identifies essential FOXO3 functions at key steps of terminal erythropoiesis, PLoS Genet. 11 (2015) e1005526.

[59] S.S. Franco, L. De Falco, S. Ghaffari, C. Brugnara, D.A. Sinclair, A. Matte, A. Iolascon, N. Mohandas, M. Bertoldi, X. An, A. Siciliano, P. Rimmelé, M.D. Cappellini, S. Michan, E. Zoratti, J. Anne, L. De Franceschi, Resveratrol accelerates erythroid maturation by activation of FoxO3 and ameliorates anemia in beta-thalassemic mice, Haematologica 99 (2014) 267–275.

[60] L. Zhang, J. Flygare, P. Wong, B. Lim, H.F. Lodish, miR-191 regulates mouse erythroblast enucleation by down-regulating Riok3 and Mxi1, Genes Dev. 25 (2011) 119–124.

[61] P. Huang, Y. Zhao, J. Zhong, X. Zhang, Q. Liu, X. Qiu, S. Chen, H. Yan, C. Hillyer, N. Mohandas, X. Pan, X. Xu, Putative regulators for the continuum of erythroid differentiation revealed by single-cell transcriptome of human BM and UCB cells, Proc. Natl. Acad. Sci. U. S. A 117 (2020) 12868–12876.

[62] M. Gothwal, J. Wehrle, K. Aumann, V. Zimmermann, A. Gründer, H.L. Pahl, A novel role for nuclear factor-erythroid 2 in erythroid maturation by modulation of mitochondrial autophagy, Haematologica 101 (2016) 1054–1064.

[63] M.-C. Xiao, N. Jiang, L.-L. Chen, F. Liu, S.-Q. Liu, C.-H. Ding, S.-H. Wu, K.-Q. Wang, Y.-Y. Luo, Y. Peng, F.-Z. Yan, X. Zhang, H. Qian, W.-F. Xie, TRIB3-TRIM8 complex drives NAFLD progression by regulating HNF4α stability, J. Hepatol. (2024) 778–791.

[64] S. Sakai, C. Miyajima, C. Uchida, Y. Itoh, H. Hayashi, Y. Inoue, Tribbles-related protein family members as regulators or substrates of the ubiquitin-proteasome system in cancer development, Curr. Cancer Drug Targets 16 (2016) 147–156.

[65] J. Fan, C.-S. Lee, S. Kim, X. Zhang, J. Pi-Anfruns, M. Guo, C. Chen, M. Rahmana, J. Li, B.M. Wu, T.L. Aghaloo, M. Lee, Trb3 controls mesenchymal stem cell lineage fate and enhances bone regeneration by scaffold-mediated local gene delivery, Biomaterials 264 (2021) 120445.

[66] M. Hernández-Quiles, R. Baak, A. Orea-Soufi, A. Borgman, S. den Haan, P. Sobrevals Alcaraz, A. Jongejan, R. van Es, G. Velasco, H. Vos, E. Kalkhoven, TRIB3 modulates pparγ-mediated growth inhibition by interfering with the MLL complex in breast cancer cells, Int. J. Mol. Sci. 23 (2022).

[67] C. Hu, Q. Li, L. Xiang, Y. Luo, S. Li, J. An, X. Yu, G. Zhang, Y. Chen, Y. Wang, D. Wang, Comprehensive pan-cancer analysis unveils the significant prognostic value and potential role in immune microenvironment modulation of TRIB3, Comput. Struct. Biotechnol. J. 23 (2024) 234–250.

[68] S. Wang, C. Wang, X. Li, Y. Hu, R. Gou, Q. Guo, X. Nie, J. Liu, L. Zhu, B. Lin, Down-regulation of TRIB3 inhibits the progression of ovarian cancer via MEK/ERK signaling pathway, Cancer Cell Int. 20 (2020) 418.

[69] M.-P. Ye, W.-L. Lu, Q.-F. Rao, M.-J. Li, H.-Q. Hong, X.-Y. Yang, H. Liu, J.-L. Kong, R.-X. Guan, Y. Huang, Q.-H. Hu, F.-R. Wu, Mitochondrial stress induces hepatic stellate cell activation in response to the ATF4/TRIB3 pathway stimulation, J. Gastroenterol. 58 (2023) 668–681.

[70] E. Ahler, W.J. Sullivan, A. Cass, D. Braas, A.G. York, S.J. Bensinger, T.G. Graeber, H.R. Christofk, Doxycycline alters metabolism and proliferation of human cell lines, PLoS One 8 (2013) e64561.

[71] Y. Xing, Z. Liqi, L. Jian, Y. Qinghua, Y. Qian, Doxycycline induces mitophagy and suppresses production of interferon-β in IPEC-J2 cells, Front. Cell. Infect. Microbiol. 7 (2017) 21.

[72] Y. Ding, L. Wang, W. Ji, Z. Chen, D. Wang, C. Chen, H. Tong, Z. Han, C. Niu, M. Chu, J. Huang, X. Guo, Generation of a human induced pluripotent stem cell line with Cas9 driven by Tet-on operator via AAVS1 safe harbor gene-editing, Stem Cell Res. 49 (2020) 102064.

[73] L.R.Z. Cohen, B. Kaffe, E. Deri, C. Leibson, M. Nissim-Rafinia, M. Maman, N. Harpaz, G. Ron, E. Shema, E. Meshorer, PRC2-independent actions of H3.3K27M in embryonic stem cell differentiation, Nucleic Acids Res. 51 (2023) 1662–1673.

[74] T. Ishida, M. Koyanagi-Aoi, D. Yamamiya, A. Onishi, K. Sato, K. Uehara, M. Fujisawa, T. Aoi, Differentiation of human induced pluripotent stem cells into testosterone-producing leydig-like cells, Endocrinology 162 (2021).

[75] X.-C. Yang, X.-L. Wu, W.-H. Li, X.-J. Wu, Q.-Y. Shen, Y.-X. Li, S. Peng, J.-L. Hua, OCT6 inhibits differentiation of porcine-induced pluripotent stem cells through MAPK and PI3K signaling regulation, Zool. Res. 43 (2022) 911–922.

[76] L. Xu, Q. Zeng, L. Liang, Z. Yang, M. Qu, H. Li, B. Zhang, J. Zhang, X. Yuan, L. Chen, Z. Fan, L. He, X. Nan, W. Yue, X. Xie, X. Pei, Generation of Rh D-negative blood using CRISPR/Cas9, Cell Prolif. 56 (2023) e13486.